 CMC, vol.52, no.1, pp.25-40, 2016

Excluded Volumes of Anisotropic Convex Particles in Heterogeneous Media: Theoretical and Numerical Studies

Wenxiang Xu[1,2,3,4], **Ganquan Yang**[5], **Peng Lan**[2], **Huaifa Ma**[1]

Abstract: Understanding the excluded volume of anisotropic particle is of great importance in the evaluation of continuum percolation and random packing behaviors of soft/hard particle systems in heterogeneous disordered media. In this work, we obtain the excluded volumes of several anisotropic convex particles including prolate spheroids, oblate spheroids, spherocylinders, and Platonic particles, using theoretical and numerical approaches. According to the second virial coefficient, we first present a theoretical scheme for determining the excluded volumes of anisotropic particles. Also, the mean tangent diameters of anisotropic convex particles are formulated by the quantitative stereology. Subsequently, Monte Carlo simulations are demonstrated to numerically evaluate the excluded volumes. The theoretical results of the dimensionless excluded volume are thereafter compared with that of the numerical results to verify the validity of the theoretical scheme. We further investigate the dependence of the dimensionless excluded volume on the geometric characteristics of anisotropic particles based on the proposed theoretical and numerical schemes. Results show that the dimensionless excluded volume mainly relies on the shape and surface information of anisotropic particles. The developed theoretical and numerical schemes can provide theoretical insights into the percolation threshold and packing density of soft/hard anisotropic particle systems in heterogeneous materials, physics, and chemistry fields.

Keywords: Excluded volume; Convex particle; Percolation, Random packing, Theory, Monte carlo simulation.

[1] State Key Laboratory of Simulation and Regulation of Water Cycle in River Basin, China Institute of Water Resources and Hydropower Research, Beijing 100048, China.
[2] Institute of Soft Matter Mechanics, College of Mechanics and Materials, Hohai University, Nanjing 210098, China
[3] State Key Laboratory of Structural Analysis for Industrial Equipment, Dalian University of Technology, Dalian 116024, China
[4] Corresponding author: Tel.: +86 25 83786873; Fax: +86 25 83736860.
E-mail address: xuwenxiang@hhu.edu.cn
[5] College of Harbour, Coastal and Offshore Engineering, Hohai University

1 Introduction

Continuum percolation and random packing behaviors of soft/hard particle systems are of high relevance of a host of material, physical, and chemistry phenomena, such as conduction and flow in porous materials, metal-insulator transition in condensed matter systems, and structure of ceramics and glasses [Stauffer and Aharony (1992); Sahimi (1994); Torquato (2002); Dong, Wang, and Yu (2015); Dugyala, Daware, and Basavaraj (2013)]. Generally, continuum percolation can result in dramatic changes in mechanical properties of composites near the percolation threshold [Sahimi (1994); Torquato (2002)]. Over the last decades, the investigation of the effective mechanical properties of composites near percolation has been broadly explored by several theoretical and numerical approaches, such as self-consistent scheme [Hill (1965)], generalized self-consistent scheme [Norris, Callegari, and Sheng (1985)], Mori-Tanaka scheme [Mori and Tanaka (1973)], differential effective medium approximation [Markov, Kazatchenko, Mousatov, and Pervago (2012)], voronoi cell numerical scheme [Dong and Atluri (2012, 2013)], and random walk numerical model [Garboczi, Synder, and Douglas (1995)].

Virtually, understandings the percolation threshold and packing density of soft/hard particles are fundamental and central tasks in the researches of continuum percolation and random packing behaviors of heterogeneous media. Considerable attention has been devoted to studying the percolation threshold and packing density of soft/hard particles with various geometries [Yi and Esmail (2012); Zhou, Zou, Pinson, and Yu (2011); Bertei, Chueh, Pharoah, and Nicolella (2014)]. For isotropic spherical particles, the packing density originated from the well-known Kepler conjecture has been theoretically and numerically confirmed equivalent to 0.74 [Kepler (1966); Hales (2005)]. Also, theoretical bounds for the percolation threshold of soft spherical particles have been recently presented by using the prototypical continuum percolation models [Torquato (2012)]. For anisotropic convex particles, the percolation threshold and packing density have also been numerically evaluated by computer simulations and achieved significant advances over the past decades [Dong, Wang, and Yu (2015); Dugyala, Daware, and Basavaraj (2013); Yi and Esmail (2012); Zhou, Zou, Pinson, and Yu (2011); Bertei, Chueh, Pharoah, and Nicolella (2014)]. However, theoretical studies for the both important properties of anisotropic particles are still unknown, further efforts should be made to design and optimize advanced heterogeneous random multiphase materials for better performance.

It has been theoretically and numerically recognized that the percolation threshold and packing density of soft/hard particles intensively depend on the excluded volume. For instance, Balberg and co-workers [Balberg, Anderson, Alexander, and Wagner (1984); Balberg (1986)] gave the general relationship between the percola-

tion threshold of soft particles as discrete pores and the excluded volume associated with soft particles for porous media, as shown in Eq. (1).

$$\phi_c = 1 - e^{-cV/V_{ex}} \tag{1}$$

where ϕ_c is the critical porosity as the percolation threshold. V and V_{ex} are the volume and the excluded volume of a discrete pore, respectively.c is a constant of order unity, which relies on the structural parameters of porous media, such as $c = 2.8$ for spherical pores, and $c = 1.4$ for spherocylinder pores. On the other hand, Williams and Philipse [Williams and Philipse (2003)] described that the random packing density of hard long spherocylinders has an inverse relation with the excluded volume. Moreover, recent work demonstrated a relationship between the packing density and the excluded volume for a homogeneous packing of hard particles using a random contact model [Gravish, Franklin, Hu and Goldman (2012)], as shown in Eq. (2).

$$\phi_f = \frac{CV}{V_{ex}} \tag{2}$$

where ϕ_f is the packing density of hard particles. C is the average number of particle contacts.

As an interesting parameter, the excluded volume of a particle characterizes the inaccessible volume to other particles. The pioneering work for the excluded volume originated from Werner Kuhn in 1934, in which the excluded volume of an object was defined as the volume around an object into which the center of another similar object is not allowed to enter if overlapping of two objects is to be avoided [Onsager (1949)]. Over the last years, theoretical and numerical efforts have been made to investigate the excluded volumes of various geometrical particles. The measurement for the excluded volume of an isotropic sphere has been well documented by employing the statistical mechanics of gases [Edwards (1965); Isihara (1950)]. An expression for the excluded volume of spheroids was proposed [Garboczi, Synder, and Douglas (1995)]. Recently, the excluded volumes of several two-/three-dimensional hyperparticles have also been investigated by theoretical approximations [Torquato and Jiao (2013); Piastra and Virga (2013)]. Alternatively, the Monte Carlo simulation also provides an effective tool for the prediction of the excluded volumes of anisotropic particles, especially for non-convex particles [Liu, Lu, Meng, Jin, and Li (2014)]. However, the direct relationships of the geometrical features of anisotropic particles and the excluded volume are not well understood yet. It is our objective in this work to address this gap.

In the present study, we theoretically and numerically derive the excluded volumes of several anisotropic convex particles including spheroid, spherocylinder, regular tetrahedron, hexahedron, octahedron, dodecahedron, and icosahedron. These

particle geometries as suitable approximations have been broadly applied to represent anisotropic discrete voids, fibers, fractures, and inclusions in the modeling researches of heterogeneous multiphase materials. The motivation of this work is to make basic upholstery for the theoretical investigations of percolation threshold and packing density of anisotropic particle systems in the near future. The rest of this article is organized as follows. In Section 2, a theoretical framework for the excluded volume is presented. In Section 3, we implement a Monte Carlo simulation to numerically estimate the excluded volume. Several theoretical and numerical results are given and discussed in Section 4. Finally, this article is completed with some concluding remarks in Section 5.

2 Theoretical framework

Supposed that two contact particles $\boldsymbol{A}$ and $\boldsymbol{B}$, and let point $\boldsymbol{C}$ be the contact point between $\boldsymbol{A}$ and $\boldsymbol{B}$. By the definition of the excluded volume illustrated above, the excluded volume of particle $\boldsymbol{A}$ can be geometrically realized from the trajectory of point $\boldsymbol{C}$ moving around $\boldsymbol{A}$. Mathematically, the excluded volume of a particle is dependent on the second virial coefficient, their relationship is expressed by the following Eqs. (3) and (4) [Kihara (1953)].

$$A_2 = \frac{N_0 V_{ex}}{2M_2^2} \tag{3}$$

$$A_2 = (4N_0 V / M_2^2) f \tag{4}$$

where A_2, N_0, and M_2 are the second virial coefficient, the Avogadro constant, and the relative molecular mass, respectively. f is a constant factor. Comparing of Eq. (3) with Eq. (4), we can find that the excluded volume of a particle relates to the particle volume and the constant factor, that is

$$V_{ex} = 8Vf \tag{5}$$

On the basis of osmotic measurement [Isihara (1950)], the constant factor f can be represented by

$$f = \frac{\bar{I}S}{8V} + \frac{1}{4} \tag{6}$$

where S and $\bar{I}$ are the surface area and mean tangent diameter of a particle, respectively. Substituting Eq. (6) into Eq. (5), the excluded volume of a particle is written as

$$V_{ex} = \bar{I}S + 2V \tag{7}$$

From Eq. (7), we can see that the excluded volume predominantly relies on the particle geometries including its volume, surface area, and mean tangent diameter. Herein, we prescribe an equivalent diameter of D_{eq} as the size of a nonspherical particle, which is defined as the diameter of a sphere having the same volume as that of the nonspherical particle [Xu and Chen (2013); Xu, Chen, and Chen (2014)]. Thus, the volume of an anisotropic geometrical particle can be written as

$$V = \frac{\pi}{6} D_{eq}^3 \tag{8}$$

On the other hand, we also define a sphericity s as the ratio between the surface area of a sphere and that of an anisotropic geometrical particle with the same volume [Xu, Duan, Ma, Chen, and Chen (2015)]. The surface area of the anisotropic particle is thus expressed as

$$S = \frac{\pi D_{eq}^2}{s} \tag{9}$$

According to the quantitative stereology [Russ and Dehoff (2000)], $\bar{I}$ of an arbitrary convex particle is displayed by

$$\bar{I} = \frac{1}{4\pi} \int \left(\frac{1}{\rho_1} + \frac{1}{\rho_2} \right) \mathrm{d}S \tag{10}$$

where ρ_1 and ρ_2 are the main curvature radii of an arbitrary point onto the particle surface. The integral is throughout the particle surface. Unfortunately, it is usually difficult to calculate ρ_1 and ρ_2 of an arbitrary convex particle. In this work, we mainly focus on common convex particles like spheroid, spherocylinder, and Platonic particles including tetrahedron, hexahedron, octahedron, dodecahedron, and icosahedron.

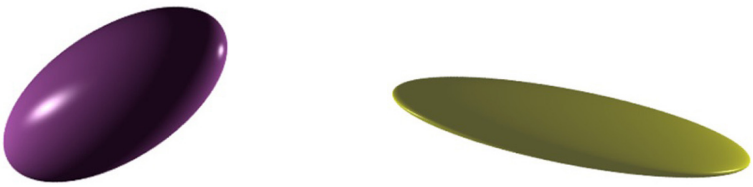

(a) (b)

Figure 1: Schematic view of a spheroid with (a) prolate shape and (b) oblate shape.

For a spheroid of an aspect ratio κ, as shown in Fig. 1, the mean tangent diameter is defined by [Dehoff and Rhines (1961)]

$$\bar{I}_e = \int_0^{\pi/2} I_e(\theta) \sin\theta \mathrm{d}\theta \tag{11}$$

where θ is the angle between the rotation axis of the spheroid and Z-axis of the Cartesian coordinate.

When $\kappa > 1$, namely, the spheroid shape is prolate, $I_e(\theta)$ is given by [Xu, Chen, Duan, and Chen (2015)]

$$I_e(\theta) = \left(a^2\cos^2\theta + c^2\sin^2\theta\right)^{1/2} \tag{12}$$

where a and c are the semi-major and semi-minor axes of the spheroid, respectively. The relationship between D_{eq} and a has been displayed as the following formula, namely,

$$D_{eq} = \begin{cases} 2a\kappa^{1/3} & \kappa < 1 \\ 2a\kappa^{-2/3} & \kappa > 1 \end{cases} \tag{13}$$

In the substitution of Eqs. (12) and (13) into Eq. (11), the mean tangent diameter of the prolate spheroid is given by

$$\bar{I}_e = \frac{1}{2}D_{eq}\left[\kappa^{2/3} + \frac{1}{\kappa^{1/3}\sqrt{\kappa^2-1}}\ln\left(\kappa+\sqrt{\kappa^2-1}\right)\right] \kappa > 1 \tag{14}$$

Similarly, when the spheroid shape is oblate, i.e., $\kappa < 1$, $I_e(\theta)$ and $\bar{I}_e$ of the oblate spheroid can be expressed as

$$I_e(\theta) = 2\left[\left(0.5D_{eq}/\kappa^{\frac{1}{3}}\right)^2\cos^2\theta + \left(0.5D_{eq}\kappa^{\frac{2}{3}}\right)^2\sin^2\theta\right]^{\frac{1}{2}} \tag{15}$$

$$\bar{I}_e = \frac{1}{2}D_{eq}\left[\kappa^{2/3} + \frac{1}{\kappa^{1/3}\sqrt{1-\kappa^2}}\arcsin\left(\sqrt{1-\kappa^2}\right)\right] \kappa < 1 \tag{16}$$

Consequently, the excluded volume of a spheroid is derived by substituting Eqs. (14) and (16) into Eq. (7), that is

$$V_{ex}^{spheroid} = \begin{cases} \left\{\frac{1}{2s}\left[\kappa^{2/3} + \frac{1}{\kappa^{1/3}\sqrt{\kappa^2-1}}\ln\left(\kappa+\sqrt{\kappa^2-1}\right)\right] + \frac{1}{3}\right\}\pi D_{eq}^3 & \kappa > 1 \\ \left\{\frac{1}{2s}\left[\kappa^{2/3} + \frac{1}{\kappa^{1/3}\sqrt{1-\kappa^2}}\arcsin\left(\sqrt{1-\kappa^2}\right)\right] + \frac{1}{3}\right\}\pi D_{eq}^3 & \kappa < 1 \end{cases} \tag{17}$$

For a spherocylinder with the aspect ratio of α, we label the height and diameter of the spherocylinder as H and D, then $\alpha = H/D$. According to the definition of equivalent diameter described above, the relation between the equivalent diameter of spherocylinder and its diameter is displayed by

$$D_{eq} = D(1+1.5\alpha)^{1/3} \tag{18}$$

On the basis of geometrical probability, the tangent diameter of spherocylinder can be given by

$$I_{spcy}(\theta) = D_{eq}(\alpha\cos\theta + 1)(1 + 1.5\alpha)^{-1/3} \tag{19}$$

As a typical rotational body, the derivation of the mean tangent diameter of spherocylinder should be similar to that of spheroid. To be specific, Eq. (11) is also suitable for the derivation of the mean tangent diameter of spherocylinder. In the substitution of Eq. (19) into Eq. (11), that is

$$\overline{I_{spcy}} = D_{eq}(0.5\alpha + 1)(1 + 1.5\alpha)^{-1/3} \tag{20}$$

Thus, the excluded volume of spherocylinder is obtained by substituting Eq. (20) into Eq. (7), as depicted in the following equation.

$$V_{ex}^{spherocylinder} = \left[\frac{1}{s}(0.5\alpha + 1)(1 + 1.5\alpha)^{-1/3} + \frac{1}{3}\right]\pi D_{eq}^3 \tag{21}$$

For Platonic particles including regular tetrahedron, hexahedron, octahedron, dodecahedron, and icosahedron, as shown in Fig.2, their mean tangent diameters no longer follow Eq. (11), since these convex polyhedra are not the bodies of revolution.

(a) (b) (c) (d) (e)

Figure 2: Schematic views of Platonic particles including (a) tetrahedron, (b) hexahedron, (c) octahedron, (d) dodecahedron, and (e) icosahedron.

Fortunately, some researches have recently reported the mean tangent diameter $\bar{I}_c$ of a convex polyhedron [Xu, Chen, Duan, and Chen (2015)], such as

$$\bar{I}_c = \frac{1}{4\pi}\sum_j (\pi - \psi_j) l_j \tag{22}$$

where j is the number of sides of a convex polyhedron. l_j and ψ_j are the side length and dihedral (i.e., the inward angle between two surfaces) corresponding to

the j side, respectively. Specifically for a regular convex polyhedron, the dihedral ψ_j for each side is the same to be ψ:

$$\psi_j = \psi = \pi - 2\text{acos}\left(\frac{\cos(\pi/f)}{\sin(\pi/n)}\right) \tag{23}$$

where f and n are the number of faces connected by each vertex and the number of sides of each face (see Tab. 1), respectively. The relationship between l_j and D_{eq} of a Platonic particle is presented by

$$D_{eq} = \frac{l_j}{b} \tag{24}$$

where b is a parameter, the value of which for each Platonic particle is presented in Table 1.

Table 1: sphericity s, the number of faces connected by each vertex f, the number of sides of each face n, the number of sides E, and the parameter b of five Platonic particles.

Platonic particle	s	f	n	E	b
tetrahedron	0.671	3	3	6	$2^{-1/6}/(2\pi)^{-1/3}$
hexahedron	0.806	3	4	12	$(6/\pi)^{-1/3}$
octahedron	0.846	4	3	12	$(2^{1.5}/\pi)^{-1/3}$
dodecahedron	0.910	3	5	30	$((22.5+15.5\times 5^{0.5})/\pi)^{-1/3}$
icosahedron	0.939	5	3	30	$((12.5+2.5\times 5^{0.5})/\pi)^{-1/3}$

In the substitution of Eqs. (23) and (24) into Eq. (22), the mean tangent diameter $\bar{I}_c$ of a Platonic particle is expressed as

$$\bar{I}_c = \frac{EbD_{eq}}{2\pi}\text{acos}\left(\frac{\cos(\pi/f)}{\sin(\pi/n)}\right) \tag{25}$$

where E is the number of sides of a Platonic particle (e.g., $E = j$, see Table 1). Consequently, substituting Eq. (25) into Eq. (7), the excluded volume of a Platonic particle can be derived by

$$V_{ex}^{Platonic} = \left[\frac{Eb}{2\pi s}\text{acos}\left(\frac{\cos(\pi/f)}{\sin(\pi/n)}\right) + \frac{1}{3}\right]\pi D_{eq}^3 \tag{26}$$

3 Numerical simulation

The excluded volume V_{ex} also can be numerically evaluated by predicting the probability P of overlap between two identical particles with random orientations and

positions in a given sampling space, of which the procedure can be realized by the Monte Carlo simulation. Without loss of generality, we first predefine a cubic cell of side length L as the sampling space. The size of cubic cell is assigned to be 40 times to the equivalent diameter of anisotropic particle to satisfying with the requirement of representative volume element (RVE). Then, we randomly generate an anisotropic particle into the cubic cell, denoted as particle i. Subsequently, a large number of identical particles are uniformly distributed into the cubic cell, the number of particles is denoted as N, and N is required to meet the reliability and efficiency of the numerical simulation. We adopt the coefficient of variation of the average statistics of P as a criterion for determining N. Herein, the coefficient of variation is set to 0.001. Furthermore, the number of valid particles overlapping with particle i is recorded as N_p. The overlap probability should thus be equivalent to the ratio of the number of valid particles to the total amount of particles, $P = N_p/N$. Consequently, the excluded volume is the product of the overlap probability and the cubic volume, $V_{ex} = PL^3$.

It should be mentioned that the critical component of operating the above procedure is to identify the inter-particle overlap. Fortunately, for anisotropic particles like ellipsoids, convex polyhedra, and spherocylinders, we have developed various numerical algorithms to check the overlap between two anisotropic particles, such as an optimal golden section search algorithm for ellipsoids [Xu and Chen (2012)], a separation axis scheme for convex polyhedra [Xu, Chen, and Liu (2013)], and a minimum distance scheme for spherocylinders [Xu, Wang, Niu, and Bai (2016)]. More details about these algorithms can be found in our previous researches.

4 Results and discussion

In order to eliminate the size effect of particle, we here define a dimensionless excluded volume as the ratio of the excluded volume to the volume of particle, as depicted in Eq. (27).

$$V_{dex} = \frac{V_{ex}}{V} \tag{27}$$

where V_{dex} is the dimensionless excluded volume. Thus, by using Eq. (27), the dimensionless excluded volumes of spheroid, spherocylinder, and Platonic particles can be respectively written as:

$$V_{dex}^{spheroid} = \begin{cases} \dfrac{3}{s}\left[\kappa^{2/3} + \dfrac{1}{\kappa^{1/3}\sqrt{\kappa^2-1}}\ln\left(\kappa+\sqrt{\kappa^2-1}\right)\right]+2 & \kappa > 1 \\ \dfrac{3}{s}\left[\kappa^{2/3} + \dfrac{1}{\kappa^{1/3}\sqrt{1-\kappa^2}}\arcsin\left(\sqrt{1-\kappa^2}\right)\right]+2 & \kappa < 1 \end{cases} \tag{28}$$

$$V_{dex}^{spherocylinder} = \frac{6}{s}(0.5\alpha+1)(1+1.5\alpha)^{-1/3}+2 \tag{29}$$

$$V_{dex}^{Platonic} = \frac{3Eb}{\pi s}\text{acos}\left(\frac{\cos(\pi/f)}{\sin(\pi/n)}\right)+2 \tag{30}$$

First of all, we investigate the theoretical and numerical results of the dimensionless excluded volume V_{dex} of spheroid by employing the above theoretical and numerical models. According to the definition of sphericity mentioned above, s can associate with κ by [Xu, Duan, Ma, Chen, and Chen (2015)]

$$s = \begin{cases} \dfrac{2\kappa^{2/3}\sin\varphi}{\sin\varphi+\kappa^2\arctan h(\sin\varphi)} & \kappa<1 \\ 1 & \kappa=1 \\ \dfrac{2\kappa^{2/3}\tan\varphi}{\tan\varphi+\kappa^2\varphi} & \kappa>1 \end{cases} \tag{31}$$

where φ is defined as $\varphi = \arccos(\eta)$ and $\eta = 1/\kappa(\kappa>1)$ or $\eta=\kappa(\kappa<1)$. Fig.3 shows that the effect of κ on V_{dex}. From Fig.3, we can see that the theoretical results of V_{dex} are in good agreement with the numerical results for different κ. It reveals that the accuracy of the present theoretical scheme for the excluded volume of spheroid is favorable. Additionally, we find that V_{dex} decreases and then increases with the increase of κ, and V_{dex} reaches the minimal value equivalent to 8.0 as $\kappa=1$ (i.e., sphere). In other words, for both oblate and prolate spheroids, V_{dex} increases as particles deviate from perfect spheres. The proposed results seem to be similar to that of effect of κ on the interfacial volume fraction around mono-/polydisperse

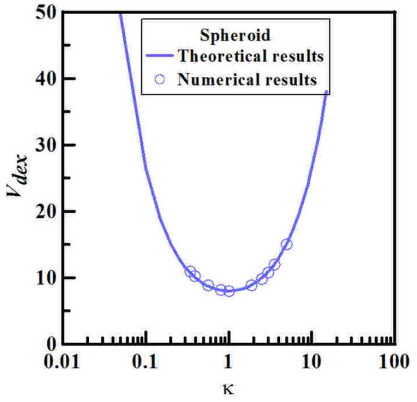

Figure 3: Effect of the aspect ratio κ of spheroid on the dimensionless excluded volume V_{dex}.

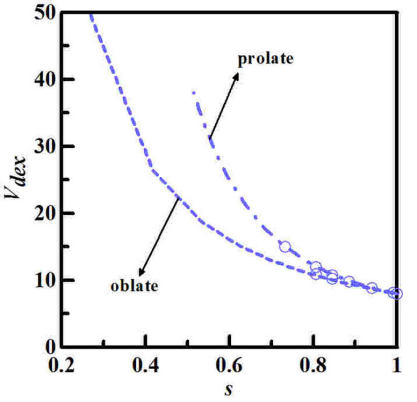

Figure 4: Effect of sphericity s of spheroid on the dimensionless excluded volume V_{dex}.

spheroids reported in recent [Xu, Chen, and Chen (2014); Xu, Duan, Ma, Chen, and Chen (2015)]. To further verify the similarity, we follow the previous studies [Xu, Duan, Ma, Chen, and Chen (2015); Xu, Chen, Duan, and Chen (2015)] that adopt sphericity s as the shape descriptor of spheroid and investigate the effect of s on V_{dex}, as shown in Fig. 4. It can be clearly seen that V_{dex} increases with the decrease of s, irrespective of oblate or prolate spheroids. Also, under the same larger s (e.g., $s > 0.88$), V_{dex} of prolate spheroid approximately equals to that of oblate spheroid. However, under the same smaller s, V_{dex} of prolate spheroid is different from that of oblate spheroid. That is to say, for the excluded volume, sphericity cannot be viewed as a shape descriptor to unify the shape of various anisotropic particles, but reflects the effect of surface configuration of particle by virtue of its concept.

Subsequently, by using the theoretical scheme and the numerical simulation, we derive the theoretical and numerical results of the dimensionless excluded volume V_{dex} of spherocylinder. Also, the relationship between sphericity s and the aspect ratio α of spherocylinder is given by

$$s = \frac{(1+1.5\alpha)^{2/3}}{1+\alpha} \tag{32}$$

Fig. 5 displays the effects of the effect of α and s on V_{dex}. As expected, Fig. 5 shows that the numerical results of V_{dex} are good consistent with that of the theoretical results for different α and s. We can see that V_{dex} increases with increasing α and with decreasing s. The proposed results present in agreement with the influence of s on the dimensionless excluded volume of spheroid shown in Fig. 4. However, it is unclear whether V_{dex} of spherocylinder is the same as that of spheroid with respect to the same s. This issue will be discussed in the following.

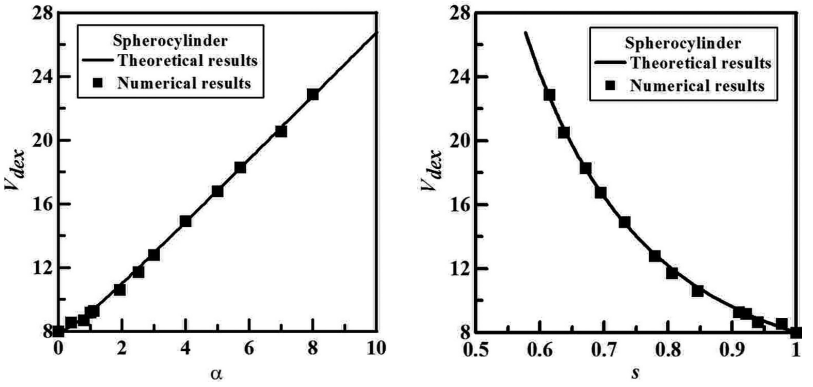

Figure 5: Effects of the aspect ratio α and sphericity s of spherocylinder on the dimensionless excluded volume V_{dex}.

Tab. 2 presents the theoretical and numerical results of V_{dex} of various anisotropic particles of various types with the same sphericity s, including five Platonic particles, prolate spheroid, oblate spheroid, and spherocylinder. For five Platonic particles, we can see from Tab. 2 that the numerical results of V_{dex} are basically consistent with that of the theoretical results. As described in Fig. 4, for the larger s (e.g., $s = 0.939$ and 0.910), Tab. 2 shows that those various anisotropic particles possess approximately the same excluded volume. For the smaller s (e.g., $s = 0.671$), the differences of V_{dex} for those anisotropic particles are significant. However, Figs. 4 and 5 and Tab. 2 show that V_{dex} decreases with the increase of s, regardless of Platonic particles, spheroid, and spherocylinder. It reveals the effect of the surface information characterized by sphericity of anisotropic convex particles on the excluded volume.

Table 2: The dimensionless excluded volumes of anisotropic particles of various types with the same sphericity, including five Platonic particles, prolate spheroid, oblate spheroid, and spherocylinder.

s		V_{dex}		prolate spheroid		oblate spheroid		spherocylinder	
		a_1	b_1	a_1	b_1	a_1	b_1	a_1	b_1
0.671	tetrahedron	15.41	15.39	18.70		13.72		18.25	18.29
0.806	hexahedron	10.99	10.93	12.11	11.96	10.73	10.96	11.98	11.71
0.846	octahedron	10.63	10.64	10.92	10.72	10.06	10.24	10.85	10.59
0.910	dodecahedron	9.12	9.03	9.42	9.35	9.11	9.16	9.39	9.26
0.939	icosahedron	8.91	8.79	8.89	8.87	8.73	8.84	8.88	8.67

a_1-theoretical results, b_1-numerical results

5 Conclusions

In this article, we described in great detail a theoretical scheme and a numerical framework to address the problem for the determination of the excluded volume of anisotropic convex particle in heterogeneous disordered media. The theoretical scheme adopted the second virial coefficient and the theories of geometrical probability and quantitative stereology. The numerical framework applied the Monte Carlo simulation for determining the overlap probability between two identical random anisotropic particles. Compared with the numerical results from the numerical framework, the theoretical scheme displayed favorable accuracy. The proposed theoretical scheme can not only be applied to calculate the excluded volumes of particles of revolution including spheroid and spherocylinder, but also to derive precisely the excluded volumes of five Platonic particles. The theoretical and nu-

merical results showed that the dimensionless excluded volume predominantly depends on the sphericity representing the surface configuration and the aspect ratio as the shape of anisotropic particle. As a significant parameter, the contribution of this article can be further drawn into theoretical investigating the percolation threshold and random packing density of soft/hard particles in discrete media.

Acknowledgement: The authors acknowledge financial supports from National Natural Science Foundation Project of China (Grant No. 11402076), Natural Science Foundation Project for Jiangsu Province (Grant No. BK20130841), China Postdoctoral Science Foundation Funded Project (Grant Nos. 2014M560385 and 2015T80493), the Open Research Fund of State Key Laboratory of Structural Analysis for Industrial Equipment (Grant No. GZ1405), the Open Research Fund of State Key Laboratory of Simulation and Regulation of Water Cycle in River Basin (Grant No. IWHR-SKL-201511), the Open Research Fund of Jiangsu Key Laboratory of Construction Materials (Grant No. CM2014-03), Jiangsu Postdoctoral Science Foundation Project (Grant No. 1402053C), and Research Special of the China Institute of Water Resources and Hydropower Research (Grant No. KY1640).

References

Balberg, I. (1986): Excluded-volume explanation of Archies law. *Phys. Rev. B*, vol. 33, no. 5, pp. 3618–3620.

Balberg, I.; Anderson, C. H.; Alexander, S.; Wagner, N. (1984): Excluded volume and its relation to the onset of percolation. *Phys. Rev. B*, vol. 30, no. 7, pp. 3933–3943.

Bertei, A.; Chueh, C.-C.; Pharoah, J. G.; Nicolella, C. (2014): Modified collective rearrangement sphere-assembly algorithm for random packings of nonspherical particles: Towards engineering applications. *Powder Technol.*, vol. 253, pp. 311–324.

Dehoff, R. T.; Rhines, F. N. (1961): Determination of number of particles per unit volume from measurements made on random plane sections: the general cylinder and the ellipsoid. *Trans. Metall. Soc. AIME*, vol. 221, pp. 975–982.

Dong, L.; Atluri, S. N. (2012): Development of 3D trefftz voronoi cells with ellipsoidal voids &/or elastic/rigid inclusions for micromechanical modeling of heterogeneous materials. *CMC: Computers, Materials & Continua*, vol. 30, no. 1, pp. 39–81.

Dong, L.; Atluri, S. N. (2013): Sgbem voronoi cells (svcs), with embedded arbitrary-shaped inclusions, voids, and/or cracks, for micromechanical modeling

of heterogeneous materials. *CMC: Computers, Materials & Continua*, vol. 33, no. 2, pp. 111–154.

Dong, K. J.; Wang, C. C.; Yu, A. B. (2015): A novel method based on orientation discretization for discrete element modeling of non-spherical particles. *Chem. Eng. Sci.*, vol. 126, pp. 500–516.

Dugyala, V. R.; Daware, S. V.; Basavaraj, M. G. (2013): Shape anisotropic colloids: synthesis, packing behavior, evaporation driven assembly, and their application in emulsion stabilization. *Soft Matter*, vol. 9 no. 29, pp. 6711–6725.

Edwards, S. F. (1965): The statistical mechanics of polymers with excluded volume. *Proc. Phys. Soc.*, vol. 85, pp. 613–624.

Garboczi, E. J.; Snyder, K. A.; Douglas, J. F. (1995): Geometrical percolation threshold of overlapping ellipsoids. *Phys. Rev. E*, vol. 52, no. 1, pp. 819–828.

Gravish, N.; Franklin, S. V.; Hu, D. L.; Goldman, D. L. (2012): Entangled granular media. *Phys. Rev. Lett.*, vol. 108, no. 20, pp. 208001.

Hales, T. C. (2005): A proof of the Kepler conjecture. *Ann. Math.*, vol. 162, no. 3, pp. 1065–1185.

Hill, R. (1965): A self-consistent mechanics of composite materials. *J. Mech. Phys. Solids*, vol. 13, no. 4, pp. 213–222.

Isihara, A. (1950): Determination of molecular shape by osmotic measurement. *J. Chem. Phys.*, vol. 18, no. 11, pp. 1446–1449.

Kepler, J. (1966): *The Six-Cornered Snowflake*. Oxford Clarendon Press.

Kihara, T. (1953): Virial coefficients and models of molecules in gases. *Rev. Mod. Phys.*, vol. 25, no. 4, pp. 831–843.

Liu, L.; Lu, P.; Meng, L.; Jin, W.; Li, S. (2014): Excluded volumes of clusters in tetrahedral particle packing. *Phys. Lett. A*, vol. 378, no. 10, pp. 835–838.

Markov, M.; Kazatchenko, E.; Mousatov, A.; Pervago, E. (2012): Generalized differential effective medium method for simulating effective elastic properties of two dimensional percolating composites. *J. Appl. Phys.*, vol. 112, no. 2, pp. 026101.

Mori, T.; Tanaka, K. (1973): Average stress in matrix and average elastic energy of materials with misfitting inclusions. *Acta Metall.*, vol. 21, no. 5, pp. 571–574.

Norris, A. N.; Callegari, A. J.; Sheng, P. (1985): A generalized differential effective medium theory. *J. Mech. Phys. Solids*, vol. 33, no. 6, pp. 525–543.

Onsager, L. (1949): The effects of shape on the interaction of colloidal particles. *Ann. N. Y. Acad. Sci.*, vol. 51, pp. 627–659.

Piastra, M.; Virga, E. G. (2013): Octupolar approximation for the excluded volume of axially symmetric convex bodies. *Phys. Rev. E*, vol. 88, no. 3, pp. 032507.

Russ, J. C.; Dehoff, R. T. (2000): *Practical Stereology*. 2nd ed., Plenum Press.

Sahimi, M. (1994): *Applications of Percolation Theory*. Taylor & Francis.

Stauffer, D.; Aharony, A. (1992): *Introduction to Percolation Theory*. Taylor & Francis.

Torquato, S. (2012): Effect of dimensionality on the continuum percolation of overlapping hyperspheres and hypercubes. *J. Chem. Phys.*, vol. 136, no. 5, pp. 054106.

Torquato, S. (2002): *Random Heterogeneous Materials: Microstructure and Macroscopic Properties*. Springer-Verlag.

Torquato, S.; Jiao, Y. (2013): Effect of dimensionality on the percolation threshold of overlapping nonspherical hyperparticles. *Phys. Rev. E*, vol. 87, no. 2, pp. 022111.

Williams, S. R.; Philipse, A. P. (2003): Random packings of spheres and spherocylinders simulated by mechanical contraction. *Phys. Rev. E*, vol. 67, no. 5, pp. 051301.

Xu, W. X.; Chen, H. S. (2012): Mesostructural characterization of particulate composites via a contact detection algorithm of ellipsoidal particles. *Powder Technol.*, vol. 221, pp. 296–305.

Xu, W. X.; Chen, H. S. (2013): Numerical investigation of effect of particle shape and particle size distribution on fresh cement paste microstructure via random sequential packing of dodecahedral cement particles. *Comput. Struct.*, vol. 114–115, pp. 35–45.

Xu, W. X.; Chen, W.; Chen, H. S. (2014): Modeling of soft interfacial volume fraction in composite materials with complex convex particles. *J. Chem. Phys.*, vol. 140, no. 3, pp. 034704.

Xu, W. X.; Chen, H. S.; Duan, Q. L.; Chen, W. (2015): Strategy for interfacial overlapping degree in multiphase materials with complex convex particles. *Powder Technol.*, vol. 283, pp. 455–461.

Xu, W. X.; Chen, H. S.; Liu, L. (2013): Evaluation of mesostructure of particulate composites by quantitative stereology and random sequential packing model of mono-/polydisperse convex polyhedral particles. *Ind. Eng. Chem. Res.*, vol. 52, no. 20, pp. 6678–6693.

Xu, W. X.; Duan, Q. L.; Ma, H. F.; Chen, W.; Chen, H. S. (2015): Interfacial effect on physical properties of composite media: Interfacial volume fraction with non-spherical hard-core-soft-shell-structured particles. *Sci. Rep.*, vol. 5, pp. 16003.

Xu, W. X.; Wang, H.; Niu, Y. Z.; Bai, J. T. (2016): Insights into interfacial effect on effective physical properties of fibrous materials. Part I: The volume fraction of soft interfaces around anisotropic fibers. *J. Chem. Phys.*, vol. 144, no. 1, pp. 014703.

Yi, Y. B.; Esmail, K. (2012): Computational measurement of void percolation thresholds of oblate particles and thin plate composites. *J. Appl. Phys.*, vol. 111, no. 12, pp. 124903.

Zhou, Z. Y.; Zou, R. P.; Pinson, D.; Yu, A. B. (2011): Dynamic simulation of the packing of ellipsoidal particles. *Ind. Eng. Chem. Res.*, vol. 50, no. 16, pp. 9787–9798.